

EVIDENCE OF THE SURFACE ORIGIN OF THE  $1/f$  NOISE

C. T. Sah\* and F. H. Hielscher\*

Department of Electrical Engineering and Materials Research Laboratory, University of Illinois, Urbana, Illinois  
(Received 19 September 1966)

The surface origin of the  $1/f$  noise power spectrum in solid-state structures has long been suspected,<sup>1</sup> although conclusive quantitative demonstration has been difficult to obtain. In this Letter we present experimental results obtained from silicon metal-oxide-semiconductor (MOS) field-effect structures. These results show both qualitative and quantitative correlations between the  $1/f$  noise-power spectrum, the lossy part of the gate impedance due to carrier recombination at the interface surface states, and the interface surface-state density over the energy band gap.

In Fig. 1, the results of these measurements for an  $N$ -channel MOS field-effect transistor structure are shown.<sup>2</sup> The upper curve,  $\rho_{SS}$ , is the density of states at the silicon-dioxide-silicon interface. This is obtained from measurement of the high-frequency capacitance versus voltage for the gate electrode which has the typical characteristics of an MOS capacitance. The shift of the experimental voltage from the zero-surface-state theoretical voltage, plotted as a function of the zero-surface-state surface potential ( $\psi_S$ ), provides the necessary information from which a graphical differentiation gives  $\rho_{SS} = (C_0/q)[d(V_{\text{exp}} - V_{\text{theory}})/d\psi_S]$ .<sup>3</sup> Here  $C_0 = K_0\epsilon_0/x_0$  is the capacitance of the gate oxide with thickness  $x_0$ . Considerable care has been taken to insure a reasonable accuracy in the differentiation by calculating the theoretical curve using several slightly different combinations of oxide thickness and substrate-impurity concentrations in the semiconductor. The variation in  $\rho_{SS}$  from each of these calculations is less than 50%. The surface potential is plotted from the theoretical calculation and shown on the upper horizontal axis of this figure where the intrinsic Fermi level,  $E_i$ , and the flat-band Fermi level,  $E_F$ , at the silicon-dioxide-silicon interface are also shown. The band edges are located at  $E_i - E_V = 22.0kT$  and  $E_C - E_i = 22.8kT$  at 300°K. This curve gives the density of interface states (states/eV-cm<sup>2</sup>) for all the states which can follow the sweep rate of the gate voltage ( $V_G$  on the bottom horizontal scale) during the capacitance-voltage measurements, a rate which was less than 10 V/min. Thus, other than those very slow

states, this measurement essentially includes all interface states. The density-of-states variation over the band gap in silicon shown in this curve is a fairly typical sample of measurements and analyses made on some 100 different types of MOS capacitors over the past three years in our laboratory.

The noise power in terms of an equivalent input resistance at the gate electrode is also shown in Fig. 1 for several frequencies. The  $1/f$  noise spectrum for this particular device was observed between 20 Hz and 100 kHz, where the lower frequency range was limited by the available wave analyzer. It is evident that the dependence of the noise power,  $R_{gn}$ , on the

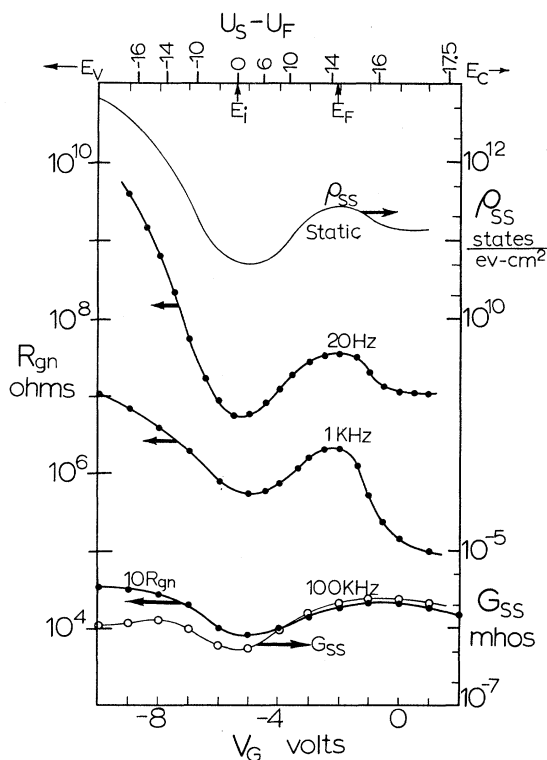


FIG. 1. The static density of surface states,  $\rho_{SS}$ , the equivalent noise resistance referred to the gate input electrode,  $R_{gn}$ , and the reduced real part of the input admittance of the gate,  $G_{SS}$ , plotted as a function of the energy in the band gap at the interface in units of  $kT/q$ ,  $U_S - U_F$ , at 300°K in an  $N$ -channel metal-oxide-silicon field-effect transistor structure. The precise definition of  $G_{SS}$  is given by the equivalent circuit shown in Fig. 2.

surface potential,  $\psi_S$  or  $V_G$ , has essentially the same structures as the total density-of-states curve,  $\rho_{SS}$ . The one-to-one correspondence is improved for the lower frequency noise power (20 Hz) as we would expect since  $\rho_{SS}$  is essentially the static curve including all states with time constant about 1 min or less while the 20-kHz noise-power curve excludes those fluctuations with time constants less than about 0.05 sec. The fact that the shape of  $R_{gn}$  for the 20-Hz case is rather similar to  $\rho_{SS}$  while there is a large difference between the 1-kHz or the 100-kHz curve and the  $\rho_{SS}$  curve indicates that there are relatively few interface states with time constants below 1/20 sec in this sample. The one-to-one correspondence between  $\rho_{SS}$  and  $R_{gn}$  in the measurements just presented are fairly typical of more than 10 samples although some of these samples have much less pronounced structures compared with this sample. The critical dependence of  $\rho_{SS}$  and  $R_{gn}$  on the fabrication processes which has been generally observed in these experiments indicates that the structure of the interface greatly influences this dependence.

A second correlation is made between the  $1/f$  noise resistance and the real part of the impedance of the gate electrode which is a measure of the recombination loss at the interface state. This is shown in the 100-kHz curves in Fig. 1 and in Fig. 2 for a second sample where somewhat more distinct structures are observed. The ratio of  $R_{gn}/G_{SS}$  for these two cases and all of the other cases is a constant over the entire band-gap energy covered in the measurements (see the upper horizontal scale in these figures). The constancy of the ratio is also plotted in the upper part of Fig. 2. Such a constancy can be readily interpreted using the Nyquist formula for resistance noise with the assumption that the interface recombination-generation mechanisms, which provide the  $1/f$  noise-power spectrum, are also the sources of the carrier recombination loss with a  $1/f$  dependence. The equivalent circuit is shown in the insert of Fig. 2 which can be used to show readily the relationship  $R_{gn}/G_{SS} = (\omega C_0)^{-2}$ .

In addition to the fine-structure correlations just presented, it has also been found that there is a proportionality relationship between the total surface-state density and the  $1/f$  noise magnitude at a low frequency such as 10 Hz for all the devices measured. Since the total

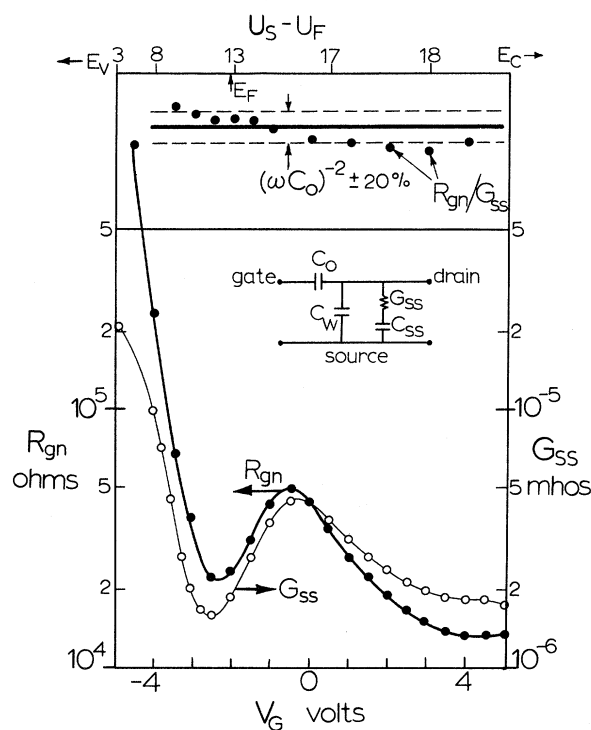


FIG. 2. The relationship between the noise resistance,  $R_{gn}$ , and the conductance of the interface states,  $G_{SS}$ , as a function of the energy in the band gap at the interface in units of  $kT/q$ ,  $U_S - U_F$ , in an  $N$ -channel MOS field-effect transistor structure. The equivalent circuit applied to the Nyquist formula to relate  $R_{gn}$  and  $G_{SS}$  is shown in the insert of this figure. In the frequency range in this paper, the approximation  $\omega C_{SS} \gg G_{SS}$  is made and the Nyquist formula  $\langle v_n^2 \rangle = 4kT\Delta f R_{SS}$  for  $G_{SS}$  is used.

surface-state density includes also those charges far away from the interface in the oxide, it appears that the interface states (or fast states) and the oxide states (or slow states) have a common origin. This has also been observed in a large number of samples directly without referring to the noise data.

A simple one-dimensional analysis<sup>4</sup> of the noise power, using a tunneling model to provide the wide distribution of time constants, shows that the observed magnitude of the  $1/f$  noise resistance requires a density of interface states for a given surface potential in excellent agreement with the density of interface states obtained from the capacitance-voltage curve such as that shown in Fig. 1.

\*Supported in part by the U. S. Air Force Office of

Scientific Research (AF-AFOSR-714-65) and the Advanced Research Projects Agency (SD-131).

<sup>1</sup>A. van der Ziel, Fluctuation Phenomena in Semiconductors (Butterworths Scientific Publications, Ltd., London, 1959), Chap. 5.

<sup>2</sup>For a review of the characteristics of the MOS field-effect transistors see C. T. Sah, IEEE Trans. Electron. Devices ED-11, 324 (1964).

<sup>3</sup>L. M. Terman, J. Solid State Electron. 5, 285 (1962).

<sup>4</sup>To be published.

## OBSERVATION OF PHONONS GENERATED IN PARAMAGNETIC RELAXATION\*

N. S. Shiren

IBM Watson Research Center, Yorktown Heights, New York

(Received 15 September 1966)

It has recently been demonstrated<sup>1</sup> that under conditions favorable for development of a phonon bottleneck, an initially inverted spin system will relax suddenly to saturation. Although this result implies formation of a phonon avalanche during the relaxation process, the phonons were not directly observed. We have now detected phonons generated at one end of an Fe<sup>2+</sup>-doped MgO rod following adiabatic rapid-passage inversion of the ground-state spin-resonance transitions. They were observed at the other end of the rod by the phonon-photon double-quantum detection technique.<sup>2</sup> Several unsuccessful attempts utilizing a similar geometry, but saturating rather than inverting the spins at the generator end of the rod, have been reported in the literature.<sup>3-5</sup> The phonon flux density in the avalanche is several orders of magnitude greater than can be obtained by saturation, and in the present experiments, also, no phonons were detected when only a saturating microwave pulse was applied; it was always necessary to have both the microwave pulse and the field sweep simultaneously present, thereby producing population inversion.

Measurements were made on several crystals, 0.3 cm diameter by 2.5-3 cm long, oriented with the rod axis parallel to the  $\langle 100 \rangle$  crystallographic direction, and containing Fe<sup>2+</sup> concentrations of about 100 ppm. In some experiments two short rods were bonded together with GE-7031 resin so as to obtain the required over-all length. The experiments were conducted at 1.9°K with the crystals immersed in the liquid He bath. Similar results were obtained on all runs. As a check to be sure that the observed effect was not due to spin saturation at the detector by electromagnetic leakage, one run was made using a doped crystal and an undoped crystal bonded together, with the latter in the generator cavity. No de-

tector pulse was obtained.

Details of the X-band inversion technique have been previously published.<sup>6</sup> The length of crystal over which the spins were inverted is determined by the microwave field configuration and is thus not sharply defined. However, it was estimated to be about 1 cm, and the distance from the end of the inversion region to the detector cavity was also about 1 cm. The double-quantum detection method has the disadvantage that its output at a given time is proportional to the phonon density integrated over the portion of the crystal ( $\geq 0.5$  cm) within the detector cavity. Its effective response time was therefore too slow to provide detailed information on the rise time of the phonon pulse. However, the method was chosen over other possibilities, such as thin-film bolometers<sup>7</sup> or Josephson junctions,<sup>8</sup> because of its frequency selectivity and its sensitivity to phonon polarization. The latter could be adjusted by changing the direction of the external magnetic field with respect to the propagation direction.

The inhomogeneously broadened Fe<sup>2+</sup> resonance is about 400 Oe wide and therefore, following rapid passage, there is a broad spectrum of inverted spin packets. However, by partially passing the line, sweeping down from high field and terminating at the dc field,  $H_0$ , only spin packets at frequencies lower than or equal to that of the microwave pulse were inverted. Then, since the Fe<sup>2+</sup> double-quantum line shape falls off sharply on the low-frequency side, it was possible to set an upper limit of about 10 MHz on the width of the phonon modes. Unfortunately, the accuracy of this result is not sufficiently great to provide a check on the theoretical prediction<sup>9</sup> that the mode width should not be larger than the homogeneous spin-packet width, estimated to be 2 MHz in our crystals.